

Detection and three-dimensional visualization of lesion models using Sonoelastography

Lawrence S. Taylor† and Thomas R. Gaborski‡ and John G. Strang§
and Deborah J. Rubens§ and Kevin J Parker†

† Electrical and Computer Engineering, University of Rochester Rochester NY

‡ Biological and Environmental Engineering, Cornell University, Ithaca NY

§ Department of Radiology, University of Rochester, Rochester NY

ABSTRACT

Sonoelastography is a vibration Doppler technique for imaging the relative elasticity of tissues. Detectability of hard lesions of various sizes has previously been demonstrated in tissue phantoms by our group. Because real tissue differs from phantom material, the injection of formaldehyde in fresh liver tissue is being used as an in-vitro lesion model. Pieces of fresh calf liver were embedded in an agar gel then injected with a bolus of 37% formaldehyde to create a stiff lesion. Two and three-dimensional sonoelastography and b-mode images were acquired. The lesions were visible in each sonoelastography image as a region of reduced vibration. After imaging, lesions were dissected and measured for size and volume. One 0.4 cc bolus injection of formaldehyde created a lesion with a volume of 10.3 cc in the sonoelastography image compared to 9.3 cc using fluid displacement of the dissected lesion. A 0.33 cc injection of formaldehyde lesion created a volume of 5 cc in the sonoelastography image compared to 4.4 cc using fluid displacement. Sonoelastography imaging techniques for imaging hard lesions in phantoms can be successfully extended to imaging formaldehyde induced lesions in real tissue.

Keywords: Sonoelastography, sonoelasticity, elastography, lesion detection, tumor, formaldehyde, calf liver, agar, lesion model

1. INTRODUCTION

Sonoelastography has been proposed as a method of imaging the relative elastic properties of soft tissues.¹ In this elastographic technique, low frequency shear wave vibrations (0 - 1000 Hz) are propagated through a region of interest while ultrasonic Doppler vibration detection methods² are used to image the resulting vibration field. Under the correct boundary conditions,^{3,4} small regions with an elevated elastic (shear or Young's) modulus relative to the surrounding material, will appear as regions of decreased vibration and the resulting vibration image will inversely correlate with the underlying distribution of the elastic modulus.

We have previously demonstrated the detectability of hard lesions in phantom materials^{5,6} using this method. One application envisioned for this imaging modality is the non-invasive real time imaging of hard tumors in the soft glandular tissues of body, such as prostate, breast and liver. Many cancerous lesions in these organs are palpably harder than the surrounding healthy tissue. Because the mechanical properties of these tissues differ from those of ultrasound phantom material, (being more non-linear and viscoelastic) we are using the injection of formaldehyde in fresh liver tissue as an *in-vitro* lesion model to validate our imaging system. The use of the term *lesion model* in this context refers to the macroscopic mechanical properties of the tissue and not to the biological structural properties of the tissue.

Prior work has been done on inducing palpably hard lesions in soft tissue. Stafford et al.⁷ used elastography to visualize thermally induced lesions *in-vitro* in soft tissue. A surgical laser was used to create thermal lesions in ovine kidney. Strain images of the kidneys revealed reduced strain levels in the lesion area as confirmed by histology. In a subsequent study at the same institution Righetti et al.⁸ used high intensity focused ultrasound

Further author information: (Send correspondence to K.J.P.)

K.J.P.: E-mail: parker@seas.rochester.edu, Telephone: 716 275 3294

to induce thermal lesions in canine livers. The strain images showing the lesion location were validated by photographs of the dissected livers. These thermal methods of inducing a lesion in soft tissue create a coagulation necrosis which is palpably harder than the untreated tissue. We have also experimented with thermal methods, applying radio frequency ablation to induce thermal lesions in bovine liver.⁹ The resulting lesions were then imaged using sonoelastography with some success. However we found that the ablation process degraded the acoustic path, reducing the quality of the both the b-mode and vibration Doppler images. Because of this we chose not to use radio frequency ablation induced thermal lesions as a model.

Formaldehyde is widely used as a fixative agent in tissue preservation. Its tissue stiffening properties are also well known. We therefore decided to investigate the injection of formaldehyde as a lesion model. To our knowledge there are no published results on imaging formaldehyde induced lesions. In this paper we described a protocol and present results for the use of formaldehyde injection into bovine liver as a lesion model for hard tumors in soft tissue. Two-dimensional (2D) and three-dimensional (3D) sonoelastography images of formaldehyde lesions are presented. Volume measurements from a fluid displacement method are compared to those of the segmented 3D sonoelastography images.

2. MATERIALS AND METHODS

Whole young bovine liver was obtained from a local butcher (Wegmans Food Markets, Rochester, NY). The liver was stored in a 0.9% NaCl solution, made from degassed H_2O , for 24 hours. 4 x 4 x 2.5 cm samples were cut from the right lobe. Samples were placed in agar molds for scanning.

Varying concentration agar molds were created to embed young bovine liver specimens. Five concentrations of DIFCO(tm) Technical Agar (Becton Dickinson, Sparks, MD) were used as the solidifying agent: 1.5%, 2.0%, 2.25%, 2.5% and 3.25% in H_2O . Increasing concentrations of agar resulted in increasing stiffness of the mold. Barium Sulfate powder ($BaSO_4$) (J.T. Baker Chemical Co., Phillipsburg, NJ) was added in three concentrations: 0.2%, 0.25% and 0.3%. The $BaSO_4$ produced background scatter in the mold, which aided in viewing the liver specimen.

The appropriate mass of agar was measured out and added to one liter of H_2O and brought to a boil with caution to avoid burning of the agar. The solution was stirred and allowed to cool to 60° C before adding $BaSO_4$ because the rate of settlement out of suspension was too fast at higher temperatures. 700 ml of the mixtures were poured into 946 ml *Ziploc*TM Tall Square Reusable-Disposable containers (S.C Johnson & Son, Racine, WI). A cylindrical container 4.5 cm in diameter was inserted 3cm at the top surface to create a cavity. The molds were then allowed to cool and stored at 4° C until used to reduce microorganism growth. The remaining 300 ml of the agar mixtures were remelted and boiled. After allowing the solutions to cool, but not harden, 15 ml was poured into the cavity before placement of one liver specimen per mold. After the specimen was placed in the cavity enough solution was added to completely embed the liver in agar.

The embedded liver molds were allowed to cool and harden before the injection of formaldehyde. 37% by weight formaldehyde solution (Fisher Scientific, Fair Lawn, NJ) was injected via hyperdermic needle in quantities of 0.40, 0.33 and 0.25 cc in the center of the liver tissues. The needle was injected into the mold at an angle of 45° to insure the needle track was not directly in the acoustic path during imaging. The plane of the injection pathway was marked with colored push pins on the surface of the agar mold to aid with locating the region of interest containing the lesion during the subsequent imaging process.

Low frequency multi-tone signals of forced vibration were applied to the specimen by placing the agar embedded samples on top of two parallel thin metal bars which were driven by a mechanical shaker. The multi-tone vibration signals served to reduced the modal artifacts which occur during *in-vitro* imaging because of specular reflection of the shear waves off of the specimen holder boundaries.¹⁰ Although each individual pure tone frequency has a pattern of destructive interference which images as a false positive for hard tissue, the patterns are uncorrelated and areas of constructive interference from one frequency fill in vibration deficits from other frequencies. The purpose of using the two parallel bars as a vibration source was twofold, to produce a uniform vibration and to focus or concentrate the shear wave production into a region of interest. The ideal vibration source in sonoelastography is one that would produce a uniform vibration field in three dimensions in a homogeneous isotropic elastic solid. The long thin bar approximates an infinite line load which is known

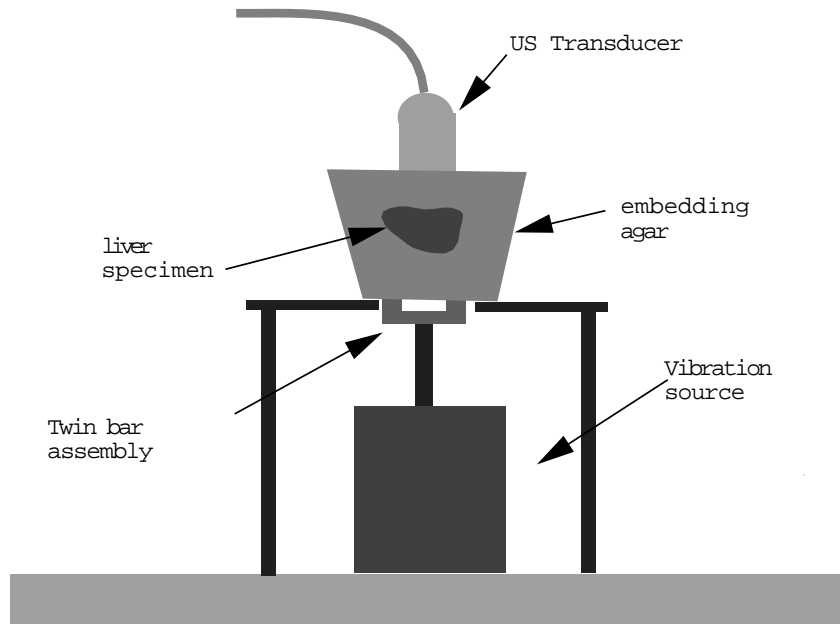


Figure 1: Experimental Set-up

to generate a state of plain strain in a homogeneous isotropic half space. We have verified theoretically and experimentally¹¹ that the twin bar arrangement focuses the shear waves produced into a region centered at the intersection of lines drawn from the bar at approximately 45° from the vertical. Figure 1 shows the experimental set-up used for scanning liver lesions. The vibration source shown is essentially a heavy duty speaker coil assembly which drives a piston shaft rather than a speaker cone. Not shown are the stereo power amplifier and the multi-tone frequency generator which supply the vibration signal.

The needle track from the bolus injection served as a visible marker allowing us to locate the formaldehyde lesion. 2D b-mode images were acquired by aligning the transducer along the needle track to insure that the lesion was at the center of the image. In order to acquire 3D b-mode and sonoelastography images a linear array transducer was mounted in a holder fixed to a motorized linear track. The specimen was positioned under the ultrasound transducer and then translated over the embedded specimen in a direction parallel to the metal bars used as the vibration source. The rate of translation was adjusted to the frame rate so that image slices were acquired 1 mm apart. Sonoelastography images were acquired by placing the specially modified scanner into the color Doppler mode in which the peak vibration amplitude is displayed as a grayscale overlay for each pixel. This is accomplished by mapping Doppler variance to the screen while suppressing any velocity estimates. In the resulting images dark gray corresponded to low vibration amplitudes and higher palpable stiffness.

After scanning, the size of a lesion was verified by removing the specimens from the embedding agar and dissecting them by cutting away the soft tissue from the palpably stiffer material. Caliper measurements were made on dissected lesion specimen to establish a minimum rectangular bounding box which would enclose the dissected lesion. The volume of each specimen was also determined by fluid displacement.

Both the 2D and 3D sonoelastography images display areas of decreased vibration as dark gray or black. The sonoelastography images of the lesions were manually segmented using the ImageJ software package from NIH. The first author outlined the vibration deficit in each image frame which suggested a lesion and used ImageJ to calculate the area of the lesion. After outlining, the lesion was filled in and the sonoelastography image was converted to a binary image where the lesion was white and the background was black. The sequence of binary 2D renderings of the lesion was imported into IRIS Explorer, a 3D visualization package to create a 3D rendering of the lesion. Since images were acquired at 1 mm intervals the volume was estimated using a cylindrical approximation multiplying the thickness of the slice by the area of the apparent lesion in each slice.

A minimum rectangular bounding box was also determined from the 3D sonoelastography by assuming its sides were either in the image plane or perpendicular to it.

3. RESULTS

Dissected lesions were basically ellipsoidal in shape except when the needle injection point was next to a liver-agar boundary. This was the case with the 0.25 cc bolus injection. A plastic film (*SaranWrapTM*) was used to surround the liver sample apparently effecting the diffusing pattern of the injected formaldehyde. The resulting lesion was observed to be gum drop shaped (a right circular cone with a smooth rather than pointed end). Lesion size increased with bolus size when the aforementioned boundary effect was eliminated. Lesions were not visible in the b-mode images but in every case were visible using sonoelastography. Measurements of three lesions are given in Table 1. In Table 1 the *caliper measurements* refer to the dissected lesion maximum dimensions and

Table 1. Lesion measurements: comparison of caliper and fluid displacement with those from the 3D sonoelastography images

Bolus size	caliper measurements	Fluid volume	image bounding box	image volume
0.40 cc	2.9 x 3.2 x 3.4 cm	9.3 cc	3.2 x 2.5 x 3.0 cm	10.3 cc
0.33 cc	2.0 x 2.0 x 2.0 cm	4.4 cc	2.2 x 2.2 x 2.3 cm	5.0 cc
0.25 cc	3.0 x 3.0 x 3.0 cm	8.3 cc	2.7 x 2.0 x 1.8 cm	4.5 cc

should be compared to the maximum dimensions observed in the sonoelastography image of the same lesion under the column heading *image bounding box*. *Fluid volume* refers to the measured volume of the dissected lesion and should be compared with the the *image volume* which was calculated from the lesion observed in the sonoelastography image.

3.1. Two-dimensional images

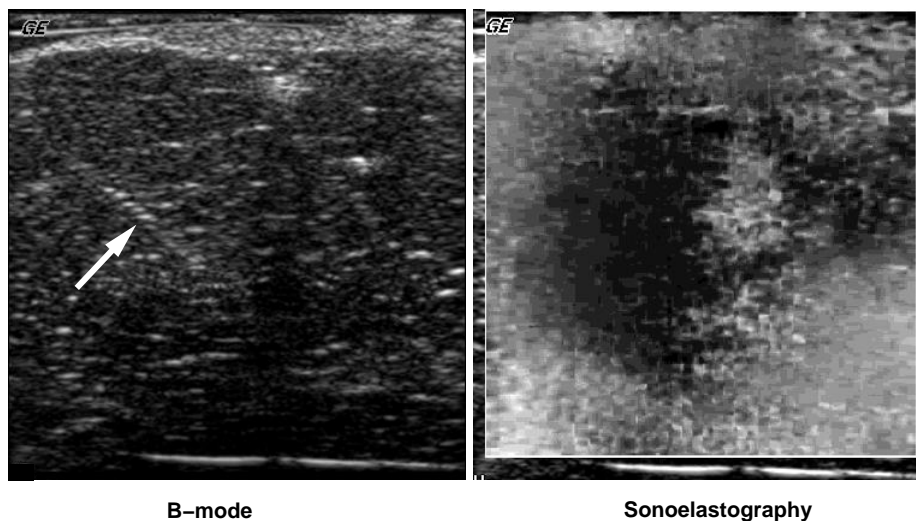


Figure 2: Images of 0.4 cc bolus lesion

Figure 2 shows the co-registered b-mode and sonoelastography images of a lesion resulting from a 0.4 cc bolus of formaldehyde. These images were taken in the plane of the needle injection as can be confirmed by the needle track visible in the b-mode image (white arrow). The field of view shown is 4 x 4 cm in both images. In

the sonoelastography image on the right the vibration amplitude has been mapped to a gray scale where high vibration is bright and low vibration is dark.

The circular or round deficit in vibration measuring about 2.5 by 2.5 cm and centered at the end of the needle track in the sonoelastography image indicates the location of the lesion. Please note that the end of the needle is near the apparent center of the vibration deficit which is what would be expected from a diffusion process uniform in all directions. The bright pixels at the right edge of the deficit are most likely artifactual, as is the portion of the vibration deficit that extends to the right edge of the image. The bright pixels are likely channel noise which is overshadowing the vibration signals in that region because of some signal attenuation. The deficit or dark gray region which goes off to the right side of the image is most likely a modal vibration node or area of destruction interference. A multi-tone signal consisting of pure tones of 128, 192 and 256 Hz was used to drive the vibration source.

Figure 3 shows the co-registered b-mode and sonoelastography images of a lesion resulting from a 0.33 cc bolus of formaldehyde. The needle track visible in the b-mode image (white arrow) confirms that these images were taken in the plane of the needle injection. The field of view shown is 4 x 5 cm in both images. In the sonoelastography image on the right the vibration amplitude has been mapped to a gray scale where high

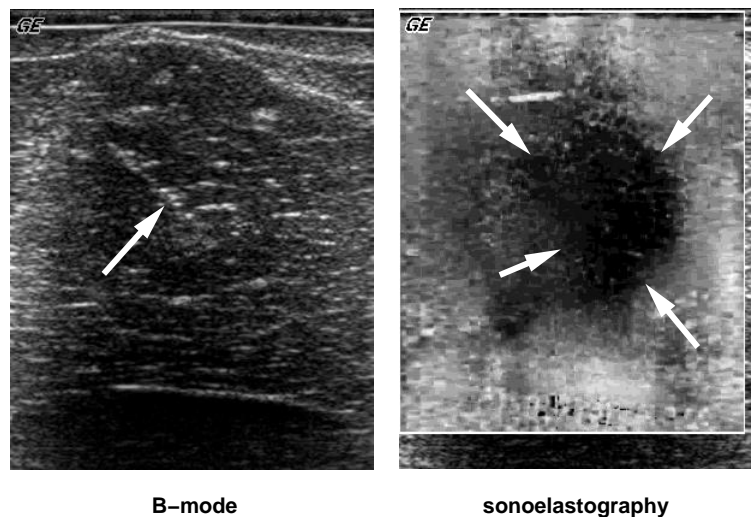


Figure 3: Images of 0.33 cc bolus lesion

vibration is bright and low vibration is dark. A vibration deficit visible in the sonoelastography image indicates the location of the lesion. It measures about 1.2 by 1.9 cm and is centered at the end of the needle track. White arrows drawn in the sonoelastography image indicate our perception of the boundary of the lesion. A multi-tone signal consisting of 152, 228 and 304 Hz pure tones was used as to drive the vibration.

Figure 4 shows the co-registered b-mode and sonoelastography images of a lesion resulting from a 0.25 cc bolus of formaldehyde. Although the needle track is not visible the images are believed to be taken in a plane through the center of the lesion. This was accomplished by using the surface markers as a guide for the transducer placement. The field of view shown is 4 x 5 cm in both images. In the sonoelastography image on the right, as in figure 2, the vibration amplitude has been mapped to a gray scale where high vibration is bright and low vibration is dark. A vibration deficit measuring about 1.2 by 1.8 cm displays the lesion in the sonoelastography image. A multi-tone signal consisting of 111, 222 and 333 Hz pure tones was used as the vibration signal. Our notes from the dissection of this lesion indicated that the lesion was gum drop shaped (conical with a rounded end) as is the vibration deficit in this image.

3.2. Three-dimensional images

Figure 5 shows a 3D sonoelastography image of a lesion resulting from a 0.33 cc bolus of formaldehyde. Each image in the sequence of 2D sonoelastography images was segmented into tumor and background, then imported into IRIS Explorer and rendered as a 3D object. The field of view shown is contained within a bounding box with sides of 2.2 x 2.2 x 2.3 cm. Pure tones of 152, 228 and 304 Hz were applied as the vibration source for imaging. Our notes from the dissection of this lesion indicate this lesion was ellipsoidal in shape which is not well captured in this image. It could be that the image resolution in the sonoelastography decreased at the edges of the lesion, accounting for the shape of the segmented lesion being closer to a cylinder than an ellipse. The volume of the lesion is given in table 1.

Figure 6 shows a 3D sonoelastography image of a lesion resulting from a 0.25 cc bolus of formaldehyde. Each image in the sequence of 2D sonoelastography images was segmented into tumor and background, then imported into IRIS Explorer and rendered as a 3D object. The field of view shown is contained with a bounding box of 2.7 x 2.0 x 1.8 cm. Pure tones of 111, 222 and 333 Hz were simultaneously applied as the vibration source. Our notes on the dissected lesion indicate this lesion was gum drop shaped (conical with rounded not pointed end), which appears to have been captured to some degree in this 3D rendering.

4. DISCUSSION

We have exploited the well known tissue stiffening properties of formaldehyde to create a lesion model for the evaluation our tumor detection system. Although phantom materials have been created which mimic the acoustical properties of human tissue it is unlikely that phantom materials will mimic their viscoelastic properties. In experiments performed by our group¹² mechanical properties of a Zerdine liver phantom were compared to those of calf liver. It was found that the calf liver had a stress relaxation an order of magnitude higher than that of Zerdine, making it a much more viscoelastic material. Creation of a lesion model was thought to be an important step towards the clinical goal of *in-vivo* tumor detection.

Little is known about the mechanical properties of the soft glandular tissues under the kind of forced vibration used in sonoelastography. Sanada and co-workers¹³ have developed and applied an ultrasound sonoelastic approach to the problem of measuring the mechanical properties of the liver *in-vivo*. Their technique exploits the fact that the velocity of shear wave propagation in an elastic medium depends on the shear modulus and density only. Using low frequency (40 Hz) shear waves on 45 normal volunteers they measured a mean velocity of 6.31 m/s in the liver, which corresponds to shear modulus of about 2.4 kPa. Catheline et al¹⁴ used transient

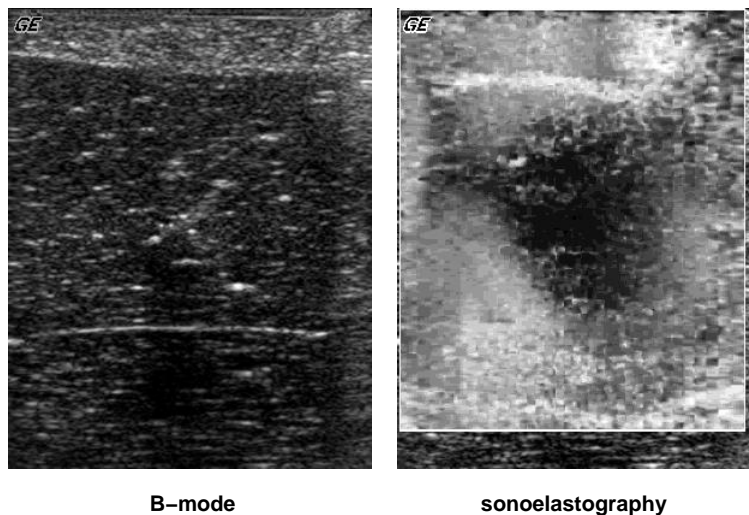


Figure 4: Images of 0.25 cc bolus lesion

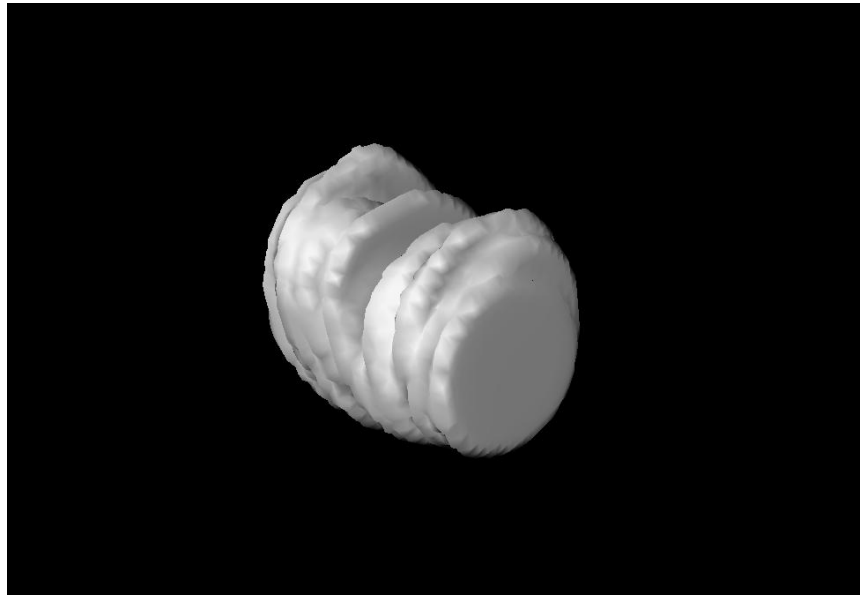


Figure 5: 3D image of 0.33 cc bolus lesion

low-frequency shear waves and measure their velocity in human biceps muscle *in-vivo*. Loading the muscle from 0 to 9 kg they measured velocities of 2 to 7.5 m/s, which corresponds to shear modulus of about 1.3 to 2.6 kPa. Arbogast and Margulies¹⁵ measured the frequency dependent shear modulus of porcine brain using a specially designed device for testing soft tissue.¹⁶ Testing adult tissue in the frequency range of 20 to 200 Hz they found the shear storage modulus varied from about 1.2 kPa to 1.8 kPa, while the shear loss modulus varied from 0.3 kPa to 2.1 kPa. It is this frequency dependent behavior, not observed in phantom material, which makes imaging a lesion model of interest. Since sonoelastography uses a range of vibration frequencies for imaging, such frequency dependent effects would impact the quality of the images. Indeed, in our prior work

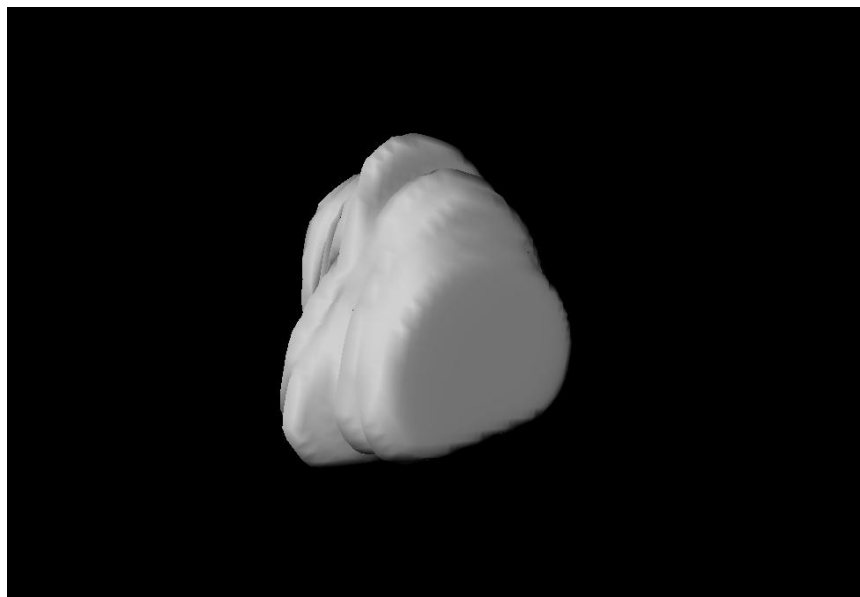


Figure 6: 3D image of 0.25 cc bolus lesion

testing liver tissue¹² we found evidence that liver follows a viscoelastic model which predicts that the shear modulus increases as the applied vibration frequency is increased, yielding results similar to those of Arbogast and Margulies.

As reported in Table 1, the agreement between the fluid displacement volume and the sonoelastography lesion volume was in the range of 10 -15% error for the resultant lesions from the 0.4 cc and 0.33 cc bolus sizes. The caliper measurements for these same lesions differed by 30 to 35%. There are several possible sources of error. While dissecting the lesions there were no visible markers as to where the lesion ended and the normal tissue began. Although the lesion could be palpated through the normal tissue there was no guarantee that the 'true' lesion boundary was found. The second author did the dissection while the first author tried to verify that only normal tissue was removed by palpating pieces of the removed tissue. The reader can easily imagine the potential for error in such a process. In fact since the injection technique creates the lesion by diffusion of formaldehyde from a point source there is no guarantee that the resulting change in material properties creates a lesion with a uniform shear modulus. A lesion whose properties vary gradually from its center to its surface would appear to be an equally plausible hypothesis. Additional mechanical tests would be required to prove or disprove either. Establishing which grayscale values in the sonoelastography image correspond to the lesion boundary would require multiple trials. For complete understanding of the lesion model, material characterization of the lesion properties as a function of frequency should be performed. We are not aware of any such studies other than the studies described in the previous paragraph.

Another source of error arises from artifacts in the sonoelastography images themselves.¹⁰ Because *in-vitro* imaging must by necessity involve finite boundaries around the specimen, vibration modes are induced which set up patterns of constructive and destructive interference. The nodes, or regions of destructive interference, mimic the areas of low vibration in sonoelastography images which indicate the lesion location. Vibration signals consisting of multiple tones (chords) were used to reduce these artifacts. It is likely that these artifacts contributed to the errors in the volume estimates in table 1. Future work on imaging these lesions should include a characterization of the modal patterns inherent in the specimen holder itself.

The discrepancy between the fluid displacement volume measurement for the 0.25 cc bolus lesion and the sonoelastography lesion is quite large. Notes from the dissection part of the experiment indicate the lesions was gum drop shaped, which is indeed confirmed by the sonoelastography image of this lesion shown in figure 4. The bolus injection protocol for this lesion differed from the other two. A thin plastic film (*SaranWrapTM*) was placed between the liver specimen and the embedding agar in order to suppress the flow of tissue fluids from the liver to the agar. This may have altered the diffusion pattern and changed how the formaldehyde altered the mechanical properties of the tissue it diffused into. In any event it was not possible to objectively determine if the elastic properties of this lesion differed from those of the other two lesions presented.

5. SUMMARY AND CONCLUSIONS

Sonoelastography imaging of palpable formaldehyde induced lesions in liver tissue has been verified. 2D sonoelastography images through the needle injection plane showed deficits of vibration centered at the end of the needle track. From this it is concluded that sonoelastography effectively detects palpably stiff lesions in soft tissue. Dissection of formaldehyde lesions verified that they were palpably harder than the surrounding tissue. Apart from palpable stiffness it was not determined whether the viscoelastic parameters of formaldehyde lesions model those of cancerous lesions in soft tissues. 3D renderings of sonoelastography detected lesions were presented. Volume estimation from these 3D images could be improved by increasing the resolution of the sonoelastography images, reducing vibration artifacts and better characterizing the lesion boundaries during the lesion dissection process. Both 2D and 3D images of the lesions have been obtained. For the larger bolus sizes volume measurements are within 20% when sonoelastography is compared to dissected measurements using an ellipsoidal shape assumption.

ACKNOWLEDGMENTS

This work was supported in part by the NSF/NYS Center for Electronic Imaging Systems, the University of Rochester Departments of Radiology and Electrical Engineering, the General Electric Company (GE) and a

grant from the NIH(2 RO1 AG16317-01A1). The authors thank GE Medical Systems Division for the loan of the Logiq 700 ultrasound scanner used in the imaging experiments.

REFERENCES

1. K. Parker, S. Huang, R. Musulin, and R. Lerner, "Tissue response to mechanical vibrations for "sonoelasticity imaging"," *Ultrasound in Med. & Biol.* **16**, pp. 241–246, 1989.
2. S. Huang, R. Lerner, and K. Parker, "On estimating the amplitude of harmonic vibrations from the doppler spectrum of reflected signals," *J Acoust Soc Am* **88**, pp. 310–317, 1990.
3. L. Gao, S. Alam, R. Lerner, and K. Parker, "Sonoelasticity imaging: Theory and experimental verification," *J Acoust Soc Am* **97**, pp. 3875–3886, 1995.
4. K. Parker, D. Fu, S. Gracewski, F. Yeung, and S. Levinson, "Vibration sonoelastography and the detectability of lesions," *Ultrasound in Med. & Biol.* **24**, pp. 1437–1447, 1998.
5. L. Taylor, B. Porter, D. Rubens, and K. Parker, "3d sonoelastography for prostate tumor imaging," in *Proceedings of the International ICSC Congress on Computational Intelligence: Methods and Applications*, pp. 468–472, ICSC Academic Press, 1999.
6. L. Taylor, B. Porter, D. Rubens, and K. Parker, "Three-dimensional sonoelastography: Principles and practices," *Physics in Medicine and Biology* **45**, pp. 1477–1494, 2000.
7. R. Stafford, F. Kallel, D. Hazle, J. Cromeens, R. Price, and J. Ophir, "Elastographic imaging of thermal lesions in soft-tissue: a preliminary study in-vitro," *Ultrasound in Med. & Biol.* **24**, pp. 1449–1458, 1998.
8. R. Righetti, F. Kallel, R. Stafford, R. Price, T. Krouskop, J. Hazle, and J. Ophir, "Elastographic characterization of hifu-induced lesions in canine livers," *Ultrasound in Med. & Biol.* **25**, pp. 1099–1113, 1999.
9. J. Strang, L. Taylor, Z. Wu, B. Porter, , D. Rubens, and K. Parker, "In-vitro imaging of rf ablation lesions in bovine liver using sonoelastography," in *Journal of Ultrasound in Medicine Official Proceedings 45th Annual Convention*, p. S:23, American Institute of Ultrasound in Medicine, 2001. Abstract only.
10. L. Taylor, D. Rubens, and K. Parker, "Artifacts and artifact reduction in sonoelastography," in *2000 IEEE Ultrasonics Symposium Proceedings*, pp. 1849–1852, IEEE, 2000.
11. Z. Wu, L. Taylor, D. Rubens, and K. Parker, "Shear wave focusing for three dimensional sonoelastography," *Journal of the Acoustical Society of America* **109**, pp. xx–xx, 2002. In Press.
12. L. Taylor, D. Rubens, and K. Parker, "Viscoelastic effects in sonoelastography: impact on tumor detectability," in *2001 IEEE Ultrasonics Symposium Proceedings*, IEEE, 2001. accepted.
13. M. Sanada, M. Ebara, H. Fukuda, M. Yoshikawa, N. Sugiura, H. Saisho, Y. Yamakoshi, K. Ohmura, A. Kobayashi, and F. Kondoh, "Clinical evaluation of sonoelasticity measurement in liver using ultrasonic imaging of internal forced low-frequency vibration," *Ultrasound in Medicine and Biology* **26**, pp. 1455–1460, 2000.
14. S. Catheline, L. Sandrin, J. Gennisson, M. Tanter, and M. Fink, "Ultrasound-based noninvasive shear elasticity probe for soft tissues," in *2000 IEEE Ultrasonics Symposium Proceedings*, pp. 1799–1801, IEEE, 2001.
15. K. Arbogast and S. Margulies, "Material characterization of the brainstem from oscillatory shear tests," *Journal of Biomechanics* **31**, pp. 801–807, 1998.
16. K. Arbogast, K. Thibault, B. Pinheiro, K. Winey, and S. Margulies, "A high-frequency shear device for testing soft biological tissues," *Journal of Biomechanics* **30**, pp. 757–759, 1997.